American Journal of Science, Engineering and Technology
2026, Vol. 11, No. 3, pp. 92–103
https://doi.org/10.11648/j.ajset.20261103.11

Research Article

Green Synthesis, Characterization, and Antimicrobial Activity of ZnO Nanoparticles Using *Zanthoxylum gilletii* Leaf Extract

Benjamin Kathoka[1, *], Kiplagat Ayabei[1], Zipporah Moraa Onyambu[1], Sharon Kiprotich[2]

[1]Department of Chemistry and Biochemistry, University of Eldoret, Eldoret, Kenya

[2]Department of Physical and Biological Sciences, Murang'a University, Murang'a, Kenya

Abstract

The green synthesis of zinc oxide (ZnO) nanoparticles has attracted significant attention as an eco-friendly alternative to conventional chemical methods. In this study, ZnO nanoparticles were synthesized using aqueous leaf extract of *Zanthoxylum gilletii*, where plant phytochemicals acted as reducing and stabilizing agents. Key synthesis parameters, including precursor concentration, reaction pH, and temperature, were systematically optimized to obtain nanoparticles with desirable physicochemical properties. Optimal synthesis conditions were achieved at 0.7 M precursor concentration, pH 10, and 60 ℃, resulting in well-defined and stable nanoparticles. The synthesized ZnO nanoparticles were characterized using UV–Visible spectroscopy, Fourier Transform Infrared (FTIR) spectroscopy, X-ray diffraction (XRD), and photoluminescence (PL) analysis. UV–Vis results showed a characteristic absorption peak at 356 nm with a band gap of 3.12 eV, confirming ZnO formation. FTIR analysis revealed a Zn–O stretching vibration at ~410 cm^{-1}, while XRD confirmed a hexagonal wurtzite structure with an average crystallite size of 29.70 nm. PL spectra exhibited an emission peak at 401 nm, indicating defect-related optical behaviour. The antimicrobial activity of the synthesized nanoparticles was evaluated against *Escherichia coli*, *Staphylococcus aureus*, *Pseudomonas aeruginosa*, and *Candida albicans* using the agar disc diffusion method. The nanoparticles exhibited significant antimicrobial activity, with mean zones of inhibition ranging from 18.67 mm to 22.00 mm. Statistical analysis (one-way ANOVA, $p > 0.05$) indicated no significant difference among the tested microorganisms, demonstrating consistent broad-spectrum antimicrobial performance. These findings demonstrate that *Zanthoxylum gilletii*-mediated green synthesis provides an effective and sustainable approach for producing ZnO nanoparticles with controlled structural and optical properties and strong antimicrobial potential.

Keywords

ZnO Nanoparticles, Green Synthesis, *Zanthoxylum Gilletii*, Nanoparticle Characterization, Antimicrobial Activity

*Correspondence: Benjamin Kathoka (benjaminmulwa536@gmail.com)

Received: 16 June 2026; **Accepted:** 26 June 2026; **Published:** 17 July 2026

Copyright: © The Author(s), 2026. Published by Science Publishing Group. This is an **Open Access** article, distributed under the terms of the Creative Commons Attribution 4.0 License (http://creativecommons.org/licenses/by/4.0/), which permits unrestricted use, distribution and reproduction in any medium, provided the original work is properly cited.

1. Introduction

In recent years, nanotechnology has gained significant attention due to the unique physicochemical properties exhibited by nanoparticles, including high surface-to-volume ratio, enhanced reactivity, and tunable optical and biological characteristics [1]. Among various metal oxide nanoparticles, zinc oxide (ZnO) nanoparticles have attracted considerable interest because of their low toxicity, chemical stability, and broad-spectrum antimicrobial activity. These properties make ZnO nanoparticles highly suitable for applications in biomedical, environmental, and food-related fields [2, 3].

Conventional methods for the synthesis of ZnO nanoparticles, such as sol–gel, hydrothermal, and chemical precipitation techniques, often involve hazardous reagents, high energy consumption, and complex processing conditions. These limitations restrict their applicability, particularly in environmentally sustainable and biomedical applications [1, 4]. As a result, there has been growing interest in the development of green synthesis approaches that utilize biological systems, especially plant extracts, as eco-friendly [2, 5].

Plant extract-mediated synthesis offers several advantages, including simplicity, cost-effectiveness, and the elimination of toxic chemicals. Phytochemical constituents such as flavonoids, phenolics, alkaloids, and terpenoids play a crucial role as reducing and stabilizing agents during nanoparticle synthesis. These biomolecules influence the nucleation, growth, and stabilization of nanoparticles, thereby affecting their size, morphology, and functional properties [5, 6]. Furthermore, plant-derived compounds can enhance the interaction between nanoparticles and microbial cells, contributing to improved antimicrobial activity [2].

Zanthoxylum gilletii, a medicinal plant widely distributed in East Africa, has traditionally been used in the treatment of infections, inflammation, and gastrointestinal disorders. The plant contains a variety of bioactive compounds with known antimicrobial and antioxidant properties [7]. Despite its established medicinal value, the application of *Zanthoxylum gilletii* in nanoparticle synthesis remains relatively underexplored compared to other plant species, highlighting its potential as a promising candidate for green nanotechnology applications [5, 6].

In addition, the increasing prevalence of antibiotic-resistant microorganisms has intensified the need for alternative antimicrobial agents. ZnO nanoparticles have demonstrated effective antimicrobial activity through multiple mechanisms, including the generation of reactive oxygen species (ROS), disruption of microbial cell membranes, and release of Zn^{2+} ions, making them strong candidates for combating microbial resistance [2, 3].

Therefore, this study aims to synthesize ZnO nanoparticles using aqueous leaf extract of *Zanthoxylum gilletii* via a green synthesis approach, optimize key synthesis parameters, and evaluate their antimicrobial activity against selected bacterial and fungal strains. The synthesized nanoparticles exhibited well-defined structural and optical properties under optimized conditions and demonstrated significant broad-spectrum antimicrobial activity, highlighting their potential for applications in biomedical and environmental fields.

2. Materials and Methods

2.1. Materials and Chemicals

All chemicals and reagents used in this study were of analytical grade and were used without further purification. Zinc nitrate hexahydrate ($Zn(NO_3)_2$ $6H_2O$) was used as the precursor for the synthesis of zinc oxide nanoparticles. Sodium hydroxide (NaOH) and hydrochloric acid (HCl) were used for pH adjustment during the synthesis process. Deionized water was used for the preparation of solutions and throughout all experimental procedures.

Fresh leaves of *Zanthoxylum gilletii* were collected from Tambach, Elgeyo Marakwet County, Kenya, and used as the biological reducing and stabilizing agent for nanoparticle synthesis. The plant material was obtained from healthy, mature plants and transported to the laboratory for further processing.

For antimicrobial analysis, nutrient agar was used for bacterial cultures, while appropriate fungal growth media were used for antifungal studies. The microbial strains tested included *Staphylococcus aureus*, *Escherichia coli*, *Pseudomonas aeruginosa*, and *Candida albicans*.

2.2. Equipment

All experimental procedures and analyses were carried out using standard laboratory equipment and advanced analytical instruments. A mechanical blender was used for the preparation of *Zanthoxylum gilletii* leaf extract, while a magnetic stirrer with a hot plate was employed for mixing and heating during nanoparticle synthesis. A pH meter was used to monitor and adjust the pH of the reaction mixture. Separation of synthesized nanoparticles was achieved using a centrifuge, followed by drying in a hot air oven and annealing in a muffle furnace.

Characterization of the synthesized ZnO nanoparticles was performed using a Thermo Scientific Evolution One Plus UV–Visible spectrophotometer (200–800 nm) to evaluate optical properties. Functional group analysis was carried out using a Shimadzu IRSpirit Fourier Transform Infrared (FTIR) spectrometer equipped with an attenuated total reflectance (ATR) accessory. Structural and phase analysis of the nanoparticles was conducted using a Thermo Scientific ARL EQUINOX 100 X-ray diffractometer (XRD).

Photoluminescence (PL) analysis was performed using an Intek SPLF97 spectrofluorometer to investigate the electronic and defect-related optical properties of the synthesized nano-

particles. Antimicrobial studies were carried out using standard microbiological equipment, including an incubator, sterile Petri dishes, and culture preparation materials.

2.3. Preparation of Plant Extract

Fresh leaves of *Zanthoxylum gilletii* were collected from Tambach, Elgeyo Marakwet County, Kenya, washed thoroughly with deionized water to remove dust and impurities, and air-dried under shade for two weeks. The dried leaves were then ground into a fine powder using a mechanical blender.

Five grams (5 g) of the powdered leaf sample were added to 500 mL of deionized water and heated at 60 ℃ for 120 minutes under constant stirring at approximately 200 rpm using a magnetic stirrer. The resulting mixture was allowed to cool to room temperature and subsequently filtered using a sieve followed by vacuum filtration to remove solid residues.

The obtained filtrate, which constituted the aqueous leaf extract, was stored at 4 ℃ and used as the reducing and stabilizing agent in the synthesis of ZnO nanoparticles.

2.4 Precursor Preparation

Zinc nitrate hexahydrate $(Zn(NO_3)_2 \cdot 6H_2O)$was used as the precursor for the synthesis of zinc oxide nanoparticles. A range of precursor solutions with varying concentrations (0.05 M, 0.1 M, 0.3 M, 0.5 M, 0.7 M, 0.9 M, and 1.0 M) was prepared by dissolving accurately weighed amounts of zinc nitrate in deionized water.

Each solution was prepared in a 100 mL volumetric flask to ensure precise concentration and homogeneity. The prepared precursor solutions were used for subsequent synthesis experiments to evaluate the effect of concentration on nanoparticle formation.

2.5. Synthesis of ZnO Nanoparticles

Zinc oxide nanoparticles were synthesized via a green synthesis approach using aqueous leaf extract of *Zanthoxylum gilletii* as a reducing and stabilizing agent. For each experiment, 30 mL of zinc nitrate precursor solution was mixed with 20 mL of the prepared plant extract in a reaction flask. The mixture was stirred continuously at 60 ℃ and heated under reflux for 2 h to reduce Zn^{2+} ions and produce ZnO nanoparticles.

After the chemical reaction, the suspension produced was centrifuged to isolate the nanoparticles that were formed. The sediment obtained was purified by washing with deionized water severally to eliminate any impurities. Annealing was done in a muffle furnace at 550 ℃ for two hours to improve the crystallinity of the sample.

Various synthesis parameters such as precursor concentration, pH of the reaction mixture, and temperature were modified for the optimization of nanoparticles. Various values for precursor concentrations between 0.05 M and 1.0 M, pH between 2 and 12, and temperatures from 30 ℃ to 90 ℃ were used individually while keeping other variables constant. Optimal conditions were obtained by using UV-Vis and FTIR analysis techniques, where information regarding the formation and stability of nanoparticles could be obtained.

Optimized synthesis conditions were found to be 0.7 M precursor concentration, pH 10 and 60 ℃ which resulted in well-defined and stable ZnO nanoparticles for further characterization and antimicrobial evaluation.

2.6. Antibacterial Evaluation Methods

The antibacterial activity of the synthesized ZnO nanoparticles was evaluated using the agar disc diffusion method against selected microbial strains, including *Staphylococcus aureus*, *Escherichia coli*, *Pseudomonas aeruginosa*, and *Candida albicans*.

Sterile nutrient agar plates were prepared and allowed to solidify under aseptic conditions. A standardized microbial suspension for each organism was uniformly spread onto the surface of the agar plates using a sterile swab to ensure even distribution of the inoculum.

Sterile filter paper discs (approximately 6 mm in diameter) were impregnated with the synthesized ZnO nanoparticle suspension and placed onto the inoculated agar surface using sterile forceps. Discs loaded with amoxicillin were used as the positive control, while discs containing deionized water served as the negative control.

The plates were incubated at 37 ℃ for 24 hours for bacterial cultures, while fungal cultures were incubated under appropriate conditions. After incubation, the zones of inhibition were measured in millimeters (mm), and the mean values were calculated from replicate experiments. The results were used to assess the antibacterial and antifungal activity of the synthesized ZnO nanoparticles.

2.7. Statistical Analysis

The antibacterial and antifungal assays were performed in triplicate, and the results were expressed as mean values ± standard deviation. Statistical analysis was conducted using one-way analysis of variance (ANOVA) to evaluate the significance of differences in the mean zones of inhibition among the tested microorganisms.

The analysis was performed using Microsoft Excel, and statistical significance was assessed at a confidence level of 95% ($p < 0.05$). The calculated F-value was compared with the critical F-value (Fcrit) to determine whether the observed differences were statistically significant. A p-value greater than 0.05 indicated no statistically significant difference among the groups.

3. Results and Discussion

3.1. Green Synthesis and Optimization of ZnO Nanoparticles

The green synthesis of ZnO nanoparticles was carried out using aqueous leaf extract of *Zanthoxylum gilletii* (Figure 1(i)), where the plant phytochemicals acted as reducing, stabilizing, and capping agents. The formation of ZnO nanoparticles was initially indicated by a visible change in the reaction mixture from a light brown solution (Figure 1(ii)) to a turbid whitish suspension (Figure 1(iii)), followed by formation of a white precipitate, which upon drying and annealing resulted in a fine white ZnO nanoparticle powder (Figure 1(iv)), suggesting the reduction of Zn^{2+} ions and nucleation of ZnO nanoparticles [8, 9].

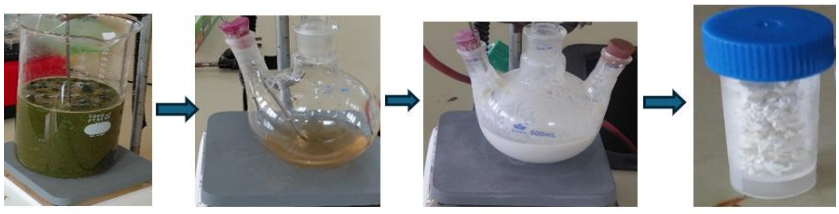

Figure 1. *Visual observation of ZnO nanoparticle synthesis showing (i) aqueous Zanthoxylum gilletii leaf extract, (ii) reaction mixture after addition of zinc nitrate precursor, (iii) formation of a turbid whitish ZnO nanoparticle suspension, and (iv) dried ZnO nanoparticles obtained after purification and annealing.*

The synthesis parameters, including precursor concentration, reaction pH, and temperature, were systematically varied to optimize nanoparticle formation. UV–Visible spectroscopy was employed to monitor nanoparticle formation through characteristic absorption peaks associated with ZnO electronic transitions. The appearance of these absorption features confirms the formation of ZnO nanoparticles and is consistent with similar observations reported in previous studies, where UV–Vis spectroscopy has been used to verify ZnO nanoparticle formation based on their characteristic optical behavior [9].

3.1.1. Effect of Precursor Concentration

The UV–Vis spectra showed that increasing precursor concentration enhanced nanoparticle formation up to an optimal level. At low concentrations (0.05–0.3 M), broad and weak absorption peaks were observed, indicating limited nucleation. At 0.7 M, a sharp and well-defined absorption peak around ~360–370 nm was obtained, indicating improved crystallinity and nanoparticle formation. At higher concentrations (0.9–1.0 M), increased baseline absorbance suggested aggregation effects [3, 4].

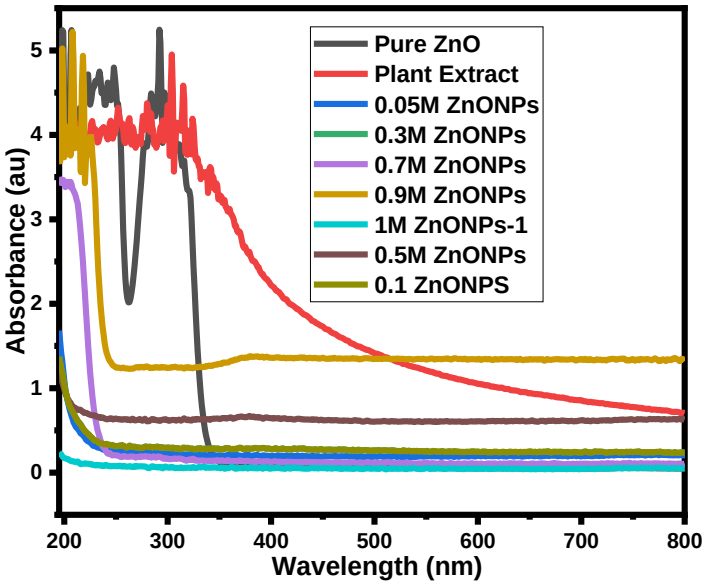

Figure 2. *UV–Vis spectra for concentration series.*

FTIR analysis further confirmed the formation of ZnO nanoparticles through the appearance of characteristic Zn–O stretching vibrations in the region of ~500–600 cm^{-1} [4, 10].

3.1.2. Effect of Reaction pH

The reaction pH significantly influenced the formation of ZnO nanoparticles. Under acidic conditions (pH 2–6), nanoparticle synthesis was suppressed due to reduced availability of hydroxide ions, leading to limited nucleation. As the pH increased, the absorption peak became more pronounced, with a distinct and well-defined characteristic peak observed at approximately 356 nm, corresponding to ZnO electronic transitions. This trend is consistent with previous studies, where increasing alkalinity enhances nanoparticle formation and leads to more defined optical absorption features associated with improved crystallinity and particle quality [11]. The pH 10 produced the most intense and well-defined UV–Vis absorption peak. This behavior is attributed to the formation of zinc hydroxide intermediates, which subsequently dehydrate to form ZnO nanoparticles [1, 2, 4]. Recent studies have shown that alkaline conditions favor ZnO nanoparticle formation by enhancing hydroxide ion availability, which promotes nucleation and growth processes, leading to improved crystallinity and particle quality [1]. In addition, recent advancements in plant-mediated synthesis highlight improved nanoparticle stability and biomedical functionality under optimized synthesis conditions [12].

At higher pH values beyond 10, slight peak broadening and reduced peak definition were observed, which may indicate aggregation of nanoparticles due to excessive nucleation and rapid growth under strongly alkaline conditions. Similar behavior has been reported in previous studies, where highly alkaline environments promote rapid particle growth and agglomeration, resulting in reduced optical definition [13]. Consequently, although higher pH enhances nanoparticle formation, pH 10 represents the optimum condition, providing a balance between nucleation, growth, and particle stability.

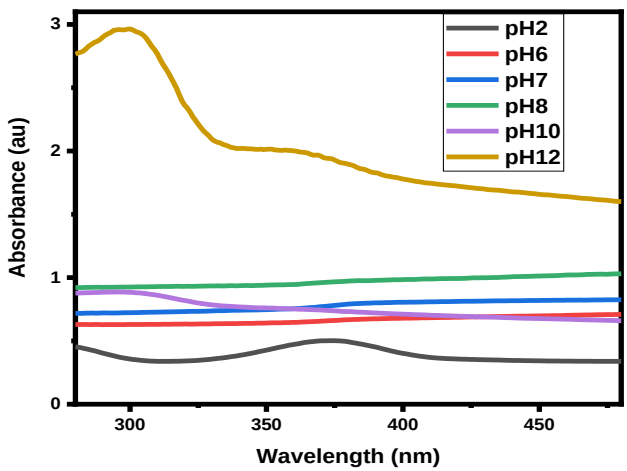

Figure 3. *UV–Vis spectra for pH variation.*

FTIR spectra at higher pH values showed stronger Zn–O bands and reduced intensity of organic functional groups, indicating improved crystallinity and reduced phytochemical interference.

3.1.3. Effect of Reaction Temperature

Temperature played a critical role in controlling nanoparticle growth and crystallinity. At lower temperatures (30–40 ℃), weak and broad absorption spectra indicated incomplete nanoparticle formation due to slower reaction kinetics. Increasing the temperature enhanced nucleation and growth, with 60 ℃ producing the sharpest absorption peak, indicative of well-defined nanoparticles. At higher temperatures, slight peak broadening suggested possible aggregation [14, 15].

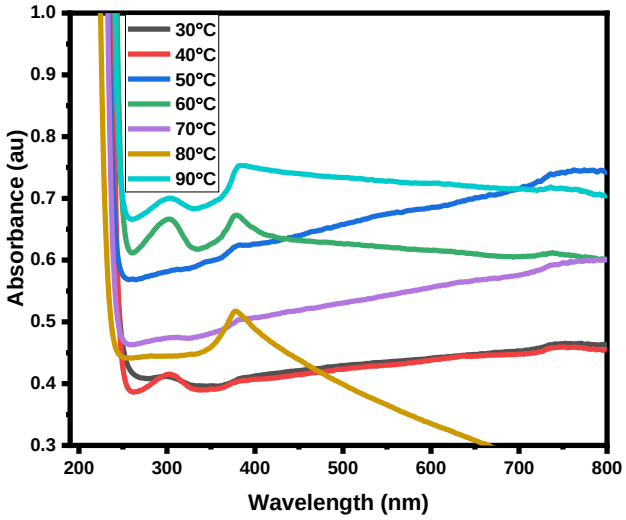

Figure 4. *UV–Vis spectra for temperature variation.*

FTIR analysis supported these results, showing increased Zn–O vibrational intensity and reduced organic residues at higher temperatures, confirming improved nanoparticle formation and purity.

The improved nanoparticle formation at 60 ℃ is attributed to enhanced reaction kinetics, which promote efficient reduction of Zn^{2+} ions and controlled growth of ZnO nuclei, resulting in improved crystallinity and particle uniformity [14, 15].

At higher temperatures, slight peak broadening was observed, suggesting possible aggregation of nanoparticles due to increased collision frequency and rapid growth rates. These findings indicate that while increasing temperature enhances nanoparticle formation, excessively high temperatures may negatively affect particle stability and dispersion.

3.1.4. Summary of Optimization

Based on the combined UV–Vis and FTIR analyses, the optimal synthesis conditions were identified as 0.7 M precursor concentration, pH 10, and a reaction temperature of 60 ℃,

which produced ZnO nanoparticles with enhanced crystallinity, stability, and minimal aggregation. These findings are consistent with previous studies reporting improved nanoparticle formation under alkaline and moderate temperature conditions [1, 2, 4].

3.2. Characterization of ZnO Nanoparticles

3.2.1. UV–Vis Analysis

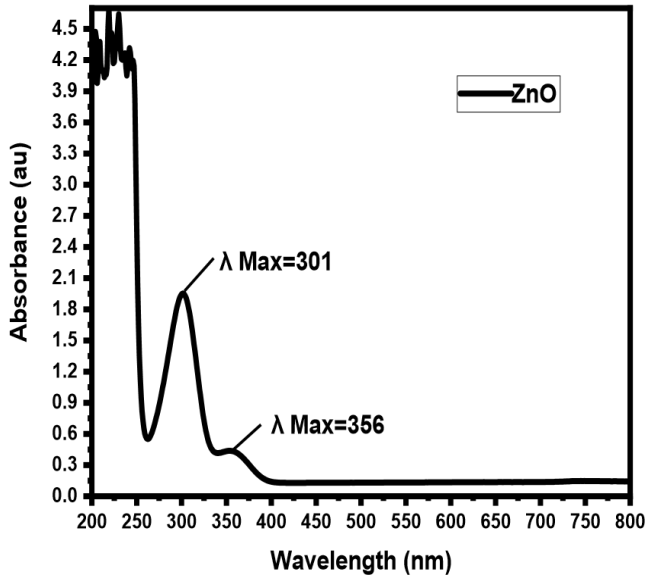

Figure 5. *UV–Visible absorption spectrum of ZnO nanoparticles showing characteristic peak at 356 nm.*

The optical properties and formation of ZnO nanoparticles were investigated using UV–Visible spectroscopy in the wavelength range of 200–800 nm. The absorption spectrum exhibited two distinct peaks at approximately 301 nm and 356 nm, which are characteristic of ZnO excitonic transitions arising from electron excitation from the valence band to the conduction band [16, 17].

The sharp absorption peak observed near 356 nm indicates the formation of well-dispersed nanoparticles with good crystallinity. A slight blue shift relative to bulk ZnO absorption behaviour suggests nanoscale particle dimensions and quantum confinement effects [18].

The optical band gap energy of the ZnO nanoparticles was determined using the Tauc plot method. The extrapolation of the linear portion of the plot yielded a band gap energy of 3.12 eV, which is slightly lower than that of bulk ZnO 3.37 eV. This reduction in band gap energy can be attributed to the presence of defect states and surface interactions with phytochemical capping agents derived from *Zanthoxylum gilletii*. These effects enhance light absorption and facilitate electron excitation, thereby improving the functional properties of the nanoparticles [18].

The optical band gap energy of the ZnO nanoparticles was determined using the Tauc plot method based on Tauc's equation:

$$(\alpha h\nu)^2 = A(h\nu - Eg)$$

where α is the absorption coefficient, $h\nu$ is the photon energy, and E_g is the band gap energy. The extrapolation of the linear portion of the plot to the energy axis yielded a band gap energy of 3.12 eV.

The observed band gap value is slightly lower than that of bulk ZnO, which can be attributed to the presence of defect states and surface interactions with phytochemical capping agents derived from *Zanthoxylum gilletii*. These effects enhance light absorption and facilitate electron excitation, thereby improving the functional properties of the nanoparticles.

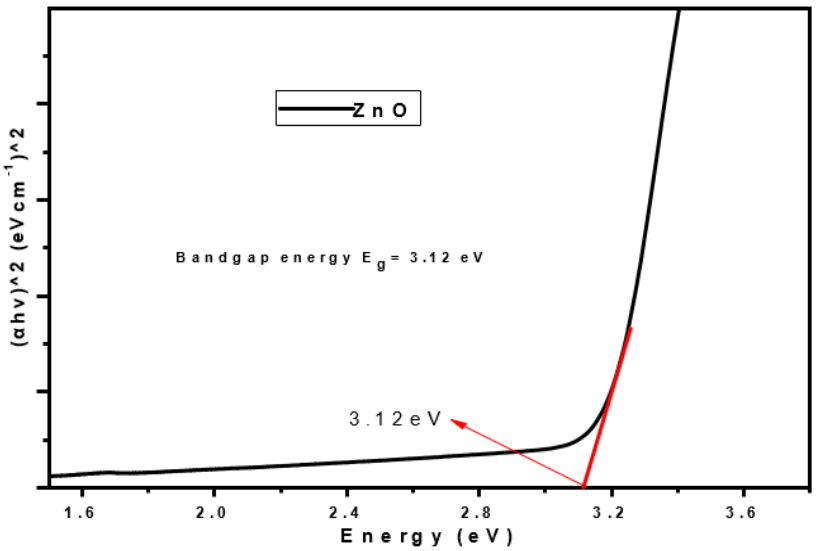

Figure 6. *Tauc plot of ZnO nanoparticles used to estimate the optical band gap energy (3.12 eV).*

The optical band gap energy (3.12 eV) obtained from the Tauc plot is slightly lower than that of bulk ZnO (3.37 eV), indicating a red shift in the absorption behaviour rather than a blue shift. This decrease in band gap energy is attributed to the presence of defect states, such as oxygen vacancies, and surface interactions with phytochemical capping agents derived from *Zanthoxylum gilletii*. These defect-related states introduce localized energy levels within the band structure, thereby reducing the effective band gap and enhancing light absorption [18].

3.2.2. FTIR Analysis

Fourier Transform Infrared (FTIR) spectroscopy was used to identify functional groups involved in nanoparticle formation and stabilization. The FTIR spectrum shows a weak and broadened absorption feature in the low wavenumber region (~400–500 cm^{-1}), with a noticeable band around ~410 cm^{-1}, which is attributed to Zn–O stretching vibrations, indicating the formation of ZnO nanoparticles. The weak intensity of this band may be due to nanoscale effects and interactions with phytochemical capping agents [4, 19].

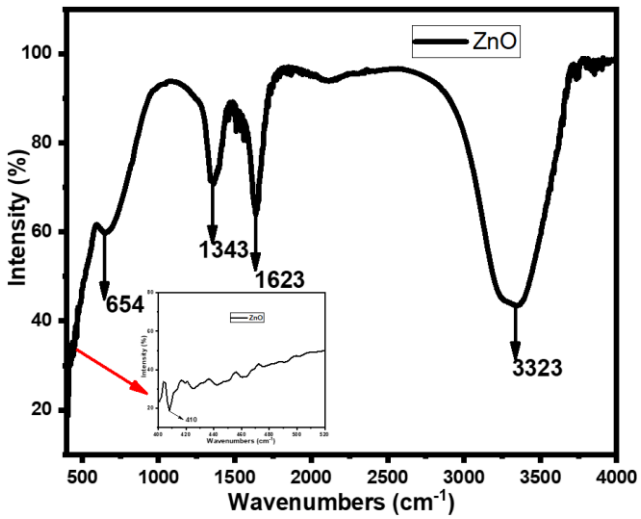

Figure 7. *FTIR spectrum of ZnO nanoparticles showing Zn–O stretching and functional groups responsible for capping and stabilization.*

A more prominent band is observed at ~654 cm^{-1}, which is not assigned to Zn–O stretching but may be attributed to other vibrational modes or Zn–O interactions influenced by plant-derived phytochemicals. Similar modifications and shifts in this region have been reported in green-synthesized ZnO systems. Additional peaks at 1623 cm^{-1} and 1343 cm^{-1} correspond to C=O and C–O stretching vibrations, respectively, while the broad band around 3323 cm^{-1} is assigned to O–H stretching vibrations. These functional groups are associated with phytochemical compounds such as flavonoids and phenolics present in the *Zanthoxylum gilletii* extract, confirming their role in nanoparticle reduction and stabilization.

These biomolecules play an essential role in the synthesis process by facilitating the reduction of Zn^{2+} ions and stabilizing the nanoparticles through capping interactions. The presence of these functional groups indicates their involvement in controlling nanoparticle nucleation, growth, and stability [2, 5, 6].

Furthermore, the presence of organic functional groups on the nanoparticle surface enhances stability and improves interaction with microbial cells, thereby contributing to the observed antimicrobial activity.

3.2.3. XRD Analysis

The crystalline structure and phase purity of the synthesized ZnO nanoparticles were investigated using X-ray diffraction (XRD). The XRD pattern exhibited well-defined diffraction peaks at 2θ values of 31.67 °, 34.08 °, 36.80 °, 47.77 °, 56.43 °, 62.73 °, and 67.82 °, corresponding to the crystallographic planes (100), (002), (101), (102), (110), (103), and (200), respectively.

These peaks are characteristic of the hexagonal wurtzite structure of ZnO nanoparticles, confirming high crystallinity and successful nanoparticle formation according to standard JCPDS data [20].

The average crystallite size was calculated using the Debye–Scherrer equation and was found to be approximately 29.70 nm, indicating nanoscale particle dimensions. The small crystallite size contributes to increased surface area and enhanced reactivity, which are important for antimicrobial performance [21].

Table 1. *XRD structural parameters of ZnO nanoparticles showing 2θ, d-spacing, β, strain, dislocation density, hkl planes, and crystallite size (D).*

2 θ Degrees	d (Å) spacing	βhkl	ε(strain) $\times 10^{-3}$	δ(nm^{-2})	hkl	D (nm)
31.67	2.82	0.16994	2.62	4.24×10^{-4}	100	48.58
34.08	2.63	0.30902	4.39	1.10×10^{-3}	002	30.13
36.80	2.44	0.33891	4.44	1.38×10^{-3}	101	26.88
47.77	1.90	0.28831	2.84	1.64×10^{-3}	102	24.71
56.43	1.63	0.49467	4.03	3.02×10^{-3}	110	18.20

The calculated average crystallite size of 29.70 nm is consistent with previously reported values for green-synthesized ZnO nanoparticles, which typically fall within the nanoscale range depending on synthesis conditions. For instance, recent studies have reported average crystallite sizes of ~28–30 nm for plant-mediated ZnO nanoparticles, closely matching the values obtained in this study [8]. This nanoscale size contributes to increased surface area and enhanced physicochemical properties, which are essential for improved antimicrobial activity [4, 21].

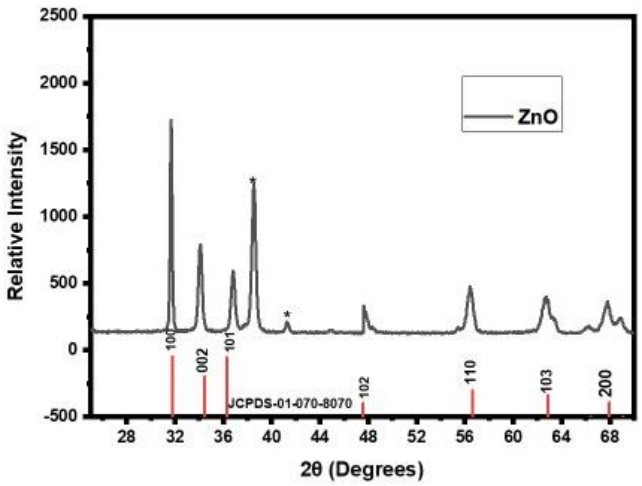

Figure 8. XRD pattern of ZnO nanoparticles confirming hexagonal wurtzite structure.

3.2.4. Photoluminescence Analysis

Photoluminescence (PL) spectroscopy was used to investigate the optical emission behaviour and defect structure of the ZnO nanoparticles. The PL spectrum exhibited three major emission peaks at approximately 401 nm, 436 nm, and 469 nm.

The strong emission peak at 401 nm corresponds to near band edge emission, indicating good crystallinity of the ZnO nanoparticles. The emission peaks at 436 nm and 469 nm are associated with defect-related emissions, particularly oxygen vacancies and zinc interstitials within the crystal lattice [22].

These defect states play a significant role in determining the optical and reactive properties of ZnO nanoparticles. In particular, they enhance chemical reactivity and contribute to antimicrobial activity through increased generation of reactive oxygen species (ROS) [23].

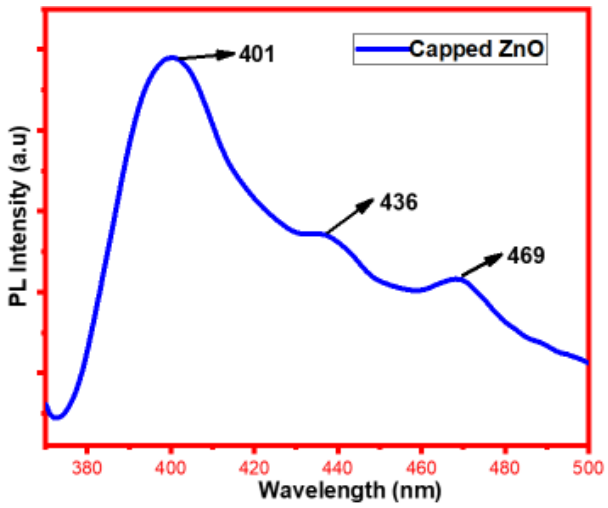

Figure 9. Photoluminescence spectrum of ZnO nanoparticles showing near band edge and defect-related emissions.

3.3. Antimicrobial Activity of ZnO Nanoparticles

The antimicrobial activity of the green synthesized ZnO nanoparticles was evaluated using the agar disc diffusion method against selected Gram-positive, Gram-negative, and fungal microorganisms, namely *Staphylococcus aureus*, *Escherichia coli*, *Pseudomonas aeruginosa*, and *Candida albicans*. The ZnO nanoparticles exhibited significant inhibitory effects against all tested organisms, as evidenced by the formation of clear zones of inhibition around the discs.

The antimicrobial activity results, including replicate measurements and mean values, are summarized in Table 2. Values are expressed as mean ± standard deviation (n = 3). Amoxicillin and fluconazole were used as positive controls for bacterial and fungal strains, respectively.

Table 2. Zones of inhibition (mm) of ZnO nanoparticles against selected microorganisms.

Microorganism	Replicate 1	Replicate 2	Replicate 3	Mean ± SD (mm)	Positive Control
Escherichia coli	17	20	19	18.67 ± 1.25	11 (Amoxicillin)
Staphylococcus aureus	18	20	21	19.67 ± 1.25	20 (Amoxicillin)
Pseudomonas aeruginosa	20	22	18	20.00 ± 1.63	12 (Amoxicillin)
Candida albicans	20	22	24	22.00 ± 1.63	14 (Fluconazole)

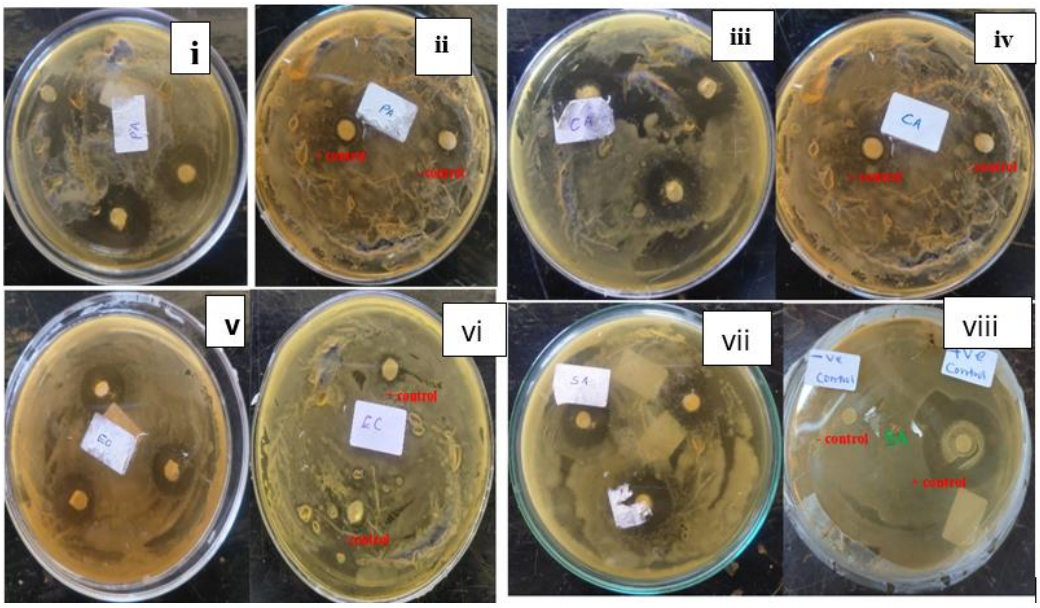

Figure 10. *Zones of inhibition produced by ZnO nanoparticles and positive control agents against (i) Pseudomonas aeruginosa treated with ZnO nanoparticles, (ii) Pseudomonas aeruginosa treated with amoxicillin, (iii) Candida albicans treated with ZnO nanoparticles, (iv) Candida albicans treated with fluconazole, (v) Escherichia coli treated with ZnO nanoparticles, (vi) Escherichia coli treated with amoxicillin, (vii) Staphylococcus aureus treated with ZnO nanoparticles, and (viii) Staphylococcus aureus treated with amoxicillin.*

The synthesized ZnO nanoparticles demonstrated strong inhibitory effects against all tested microorganisms, with the highest antimicrobial activity observed against *Candida albicans*, followed by *Pseudomonas aeruginosa*, *Staphylococcus aureus*, and *Escherichia coli*. These results indicate the broad-spectrum antimicrobial activity of the nanoparticles.

The variation in antimicrobial activity among the tested organisms may be attributed to differences in cell wall structure and composition. Gram-negative bacteria such as *E. coli* and *P. aeruginosa* possess an outer membrane that can influence nanoparticle penetration, whereas Gram-positive bacteria such as *S. aureus* have a thicker peptidoglycan layer. The relatively higher susceptibility of *Candida albicans* suggests enhanced interaction between ZnO nanoparticles and fungal cell membranes [2].

When compared with the positive controls, amoxicillin for bacteria and fluconazole for fungi, the synthesized ZnO nanoparticles exhibited comparable and, in some cases, superior antimicrobial activity, particularly against *Pseudomonas aeruginosa* and *Candida albicans*. The negative control (deionized water) showed no inhibitory effect, confirming that the observed antimicrobial activity was solely attributed to the ZnO nanoparticles.

The antimicrobial action of ZnO nanoparticles is attributed to several synergistic mechanisms. These include the generation of reactive oxygen species (ROS), which induce oxidative stress and damage cellular components such as lipids, proteins, and DNA, as well as direct interaction with microbial cell membranes, leading to increased permeability, membrane disruption, and eventual cell lysis [2, 3].

Furthermore, the nanoscale crystallite size (~29.70 nm) and defect structures identified through XRD and photoluminescence analyses enhance surface reactivity and promote ROS generation, thereby improving antimicrobial efficiency.

Statistical evaluation using one-way ANOVA indicated a p-value greater than 0.05, demonstrating that there was no statistically significant difference in antimicrobial activity among the tested microorganisms. This suggests that the synthesized ZnO nanoparticles exhibit consistent and effective antimicrobial activity against both bacterial and fungal species.

4. Conclusions

The present study successfully demonstrated the green synthesis of ZnO nanoparticles using aqueous leaf extract of *Zanthoxylum gilletii* as both a reducing and stabilizing agent. The synthesis parameters were optimized, with optimal conditions identified as a precursor concentration of 0.7 M, pH 10, and a reaction temperature of 60 ℃, resulting in well-defined and stable nanoparticles.

Characterization results confirmed the successful formation of ZnO nanoparticles with desirable physicochemical properties. UV–Visible analysis revealed a characteristic absorption peak corresponding to a band gap energy of 3.12 eV, while FTIR analysis confirmed Zn–O bond formation and the presence of functional groups involved in nanoparticle stabilization. XRD analysis established a hexagonal wurtzite crystalline structure with an average crystallite size of 29.70 nm, and photoluminescence studies indicated defect states associated with enhanced surface reactivity. The synthesized ZnO nanoparticles exhibited significant broad-spectrum antimicrobial

activity against both bacterial (*Escherichia coli*, *Staphylococcus aureus*, *Pseudomonas aeruginosa*) and fungal (*Candida albicans*) pathogens, with inhibition zones comparable to, and in some cases exceeding, those of standard antimicrobial agents. This activity is attributed to their nanoscale size, high surface area, structural defects, and the generation of reactive oxygen species.

Overall, the findings demonstrate that *Zanthoxylum gilletii*-mediated ZnO nanoparticles provide an eco-friendly, cost-effective, and efficient approach for producing potent antimicrobial agents, with promising potential for applications in biomedical and environmental fields.

Future research should focus on evaluating the long-term toxicity and biocompatibility of the synthesized ZnO nanoparticles for safe biomedical applications. Additionally, further studies may explore large-scale synthesis, detailed mechanistic investigations of antimicrobial activity, and the integration of these nanoparticles into practical applications such as water treatment, drug delivery systems, and antimicrobial coatings.

Abbreviations

ZnO	Zinc Oxide
UV–Vis	Ultraviolet–Visible Spectroscopy
FTIR	Fourier Transform Infrared Spectroscopy
XRD	X-ray Diffraction
PL	Photoluminescence
ROS	Reactive Oxygen Species
NPs	Nanoparticles

Acknowledgments

The authors acknowledge the department of Physical and Biological Sciences, Murang'a University of Technology, for providing the laboratory facilities for this study. The authors also appreciate the assistance provided by the laboratory staff during the experimental work.

Author Contributions

Benjamin Kathoka: Conceptualization, Data curation, Formal Analysis, Investigation, Methodology, Writing – original draft

Kiplagat Ayabei: Supervision, Validation, Writing – review & editing

Zipporah Moraa Onyambu: Data curation, Formal Analysis, Visualization

Sharon Kiprotich: Validation, Writing – review & editing

Funding

This work is not supported by any external funding.

Data Availability Statement

The data supporting the outcome of this research work has been reported in this manuscript.

Conflicts of Interest

The authors declare no conflicts of interest.

References

[1] Ibrahim Khan KS, Khan I. Nanoparticles: Properties, applications and toxicities. Arab J Chem. 2019; 12(7): 908–31. https://doi.org/10.1016/j.arabjc.2017.05.011

[2] Sirelkhatim A, Mahmud S, Seeni A, Kaus NHM, Ann LC, Bakhori SKM, et al. Review on zinc oxide nanoparticles: antibacterial activity and toxicity mechanism. Nano-Micro Lett. 2015; 7(3): 219–42. https://doi.org/10.1007/s40820-015-0040-x

[3] Raghupathi KR, Koodali RT, Manna AC. Size-dependent bacterial growth inhibition and mechanism of antibacterial activity of zinc oxide nanoparticles. Langmuir. 2011; 27(7): 4020–8. https://doi.org/10.1021/la104825u

[4] Kołodziejczak-Radzimska A, Jesionowski T. Zinc oxide—from synthesis to application: a review. Materials. 2014; 7(4): 2833–81. https://doi.org/10.3390/ma7042833

[5] Iravani S. Green synthesis of metal nanoparticles using plants. Green Chem. 2011; 13(10): 2638–50. https://doi.org/10.1039/C1GC15386B

[6] Ahmed S, Ahmad M, Swami BL, Ikram S. A review on plants extract mediated synthesis of silver nanoparticles for antimicrobial applications: a green expertise. J Adv Res. 2016; 7(1): 17–28. https://doi.org/10.1016/j.jare.2015.02.007

[7] Wekesa EN, Kimani NM, Kituyi SN, Omosa LK, Santos CB. Therapeutic potential of the genus Zanthoxylum phytochemicals: A theoretical ADME/Tox analysis. South African Journal of Botany. 2023 Nov 1; 162: 129-41. https://doi.org/10.1016/j.sajb.2023.09.009

[8] Al-Harbi HF, Awad MA, Ortashi KM, Al-Humaid LA, Ibrahim AA, Al-Huqail AA. Green synthesis of zinc oxide nanoparticles: physicochemical Characterization, photocatalytic Performance, and evaluation of their impact on seed germination parameters in crops. Catalysts. 2025; 15(10): 924. https://doi.org/10.3390/catal15100924

[9] Alqahtani OS, Muddapur UM, Kamat K, Shenvi A, Shaikh IA, Aljaezi I, Al Kazman BS, Alshamrani MA, Khan AA, Al-Qahtani AM, Mannasaheb BA. Sustainable green synthesis of zinc oxide nanoparticles utilizing Zingiber officinale peel aqueous extract, characterization, and determination of its anticancer and antimicrobial potential. PLoS One. 2025 Nov 19; 20(11): e0334685. https://doi.org/10.1371/journal.pone.0334685

[10] Lestari D, Masriaha I, Hasibuana AYP, Pratiwi PB. FTIR Analysis of ZnO-Functionalized Activated Carbon Derived from Oil Palm Empty Fruit Bunches for Potential Photocatalytic Applications. J Bio-Geo Mater Dan Energi. 2026; 6(1): 51–7. https://doi.org/10.22437/j-bigme.v6i1.49493

[11] Aouadi A, Hamada Saud D, Rebiai A, Achouri A, Benabdesselam S, Mohamed Abd El-Mordy F, et al. Introducing the antibacterial and photocatalytic degradation potentials of biosynthesized chitosan, chitosan–ZnO, and chitosan–ZnO/PVP nanoparticles. Sci Rep. 2024; 14(1): 14753. https://doi.org/10.1038/s41598-024-65579-z

[12] Ravi P, Babu S. Recent development in plant-mediated zinc oxide nanoparticles with biomedical applications. Chem Phys Impact. 2025; 10: 100870. https://doi.org/10.1016/j.chphi.2025.100870

[13] López-López JR, Hernández-Chávez MA, López-López M de J, Tejeda-Ochoa A, Cervantes-Gaxiola ME, Parra-Unda JR, et al. Tagetes erecta—mediated green synthesis of ZnO–Ag nanocomposites: characterization and dual applications in solar photocatalytic degradation and antibacterial activity. Ceramics. 2025; 8(2): 45. https://doi.org/10.3390/ceramics8020045

[14] Harish V, Ansari MM, Tewari D, Gaur M, Yadav AB, García-Betancourt ML, et al. Nanoparticle and nanostructure synthesis and controlled growth methods. Nanomaterials. 2022; 12(18): 3226. https://doi.org/10.3390/nano12183226

[15] Dejene F. Characterization of low-temperature-grown ZnO nanoparticles: The effect of temperature on growth. J Phys Commun. 2022; 6(7): 075011. https://doi.org/10.1088/2399-6528/ac8049

[16] Jamdagni P, Khatri P, Rana JjjS. Green synthesis of zinc oxide nanoparticles using flower extract of Nyctanthes arbor-tristis and their antifungal activity. J King Saud Univ-Sci. 2018; 30(2): 168–75. https://doi.org/10.1016/j.jksus.2016.10.002

[17] Ifeanyichukwu UL, Fayemi OE, Ateba CN. Green synthesis of zinc oxide nanoparticles from pomegranate (Punica granatum) extracts and characterization of their antibacterial activity. Molecules. 2020; 25(19): 4521. https://doi.org/10.3390/molecules25194521

[18] Kamarajan G, Anburaj DB, Porkalai V, Muthuvel A, Nedunchezhian G, Mahendran N. Green synthesis of ZnO nanoparticles and their photocatalyst degradation and antibacterial activity. 2022. https://doi.org/10.22090/jwent.2022.02.006

[19] Ullah S, Gulnaz A, Anwar S, Kamal A, Wali H. Synthetization and characterization of zinc oxide nanoparticles by X-ray diffractometry (XRD), fourier transforms, infra-red spectroscopy (FT-IR), scanning electron microscopy (SEM) and antibacterial activity test. Am J Phys Sci. 2024; 2(1): 1–25. https://doi.org/10.47604/ajps.2294

[20] Jepngetich J, Njoroge PW, Opiyo S, Kiprotich S. Synthesis and characterization of Ag-ZnO using citrus reticulata peel extract. Mater Res Express. 2025; 12(5): 055003. https://doi.org/10.1088/2053-1591/adda91

[21] Basak S, Sikdar S, Ali S, Mondal M, Haydar MS, Sarkar K, et al. Rational synthesis and characterization of temperature switching ZnFe 2 O 4/ZnO nanocomposites used for anti-bacterial, anti-oxidant and seed germination properties. New J Chem. 2024; 48(8): 3624–37. https://doi.org/10.1039/D3NJ04160C

[22] Chitradevi T, Jestin Lenus A, Victor Jaya N. Structure, morphology and luminescence properties of sol-gel method synthesized pure and Ag-doped ZnO nanoparticles. Mater Res Express. 2020; 7(1): 015011. https://doi.org/10.1088/2053-1591/ab5c53

[23] Abebe B, Zereffa EA, Tadesse A, Murthy HA. A review on enhancing the antibacterial activity of ZnO: Mechanisms and microscopic investigation. Nanoscale Res Lett. 2020; 15(1): 190. https://doi.org/10.1186/s11671-020-03418-6

Biography

Benjamin Kathoka is a postgraduate student in the Department of Chemistry and Biochemistry at the University of Eldoret, Kenya. He holds a bachelor's degree in chemistry and is currently pursuing a Master's degree with a focus on nanotechnology and green synthesis of metal oxide nanoparticles. His research interests include nanoparticle synthesis, characterization techniques, and antimicrobial applications of nanomaterials. He has been involved in experimental research focusing on environmentally friendly approaches to nanomaterial production. His current work centers on the synthesis and evaluation of ZnO nanoparticles using plant-mediated methods for biomedical and environmental applications.

Kiplagat Ayabei is a lecturer in the Department of Chemistry and Biochemistry at the University of Eldoret, Kenya. He holds a PhD. in Chemistry and is actively involved in research and teaching in analytical and materials chemistry. His research interests include nanomaterials, environmental chemistry, and sustainable synthesis methods. He has supervised several undergraduate and postgraduate research projects and contributes to academic development through mentorship and research guidance.

Zipporah Moraa Onyambu is a Doctor of Analytical Chemistry from the University of Eldoret, specializing in food security, nutrition, and cosmetic product analysis. Her research focuses on the bioaccessibility of key nutrients, such as Vitamin B and beta-carotene, in thermally processed African indigenous vegetables, contributing to improved dietary insights and food security. She has also examined the safety of cosmetic products in Kenya, particularly studying heavy metal levels in aloe vera-based creams, soaps, and skincare products. Her work highlights potential health risks and supports stronger quality standards in the cosmetics industry. Dr. Onyambu has authored several peer-reviewed articles and a master's thesis, with her research gaining academic citations. She continues to contribute to advancing knowledge in analytical chemistry, public health, and consumer safety.

Sharon Kiprotich is the Head of the Department (HOD) of Physical and Biological Sciences at Murang'a University of Technology, Kenya. She holds a PhD in Physics and has extensive experience in interdisciplinary research bridging physical and biological systems. Her research focuses on applied physics, nanomaterials, and materials science, with particular emphasis on the structural, optical, and luminescence properties of nanoparticles such as cadmium telluride (CdTe) quantum dots and zinc oxide (ZnO) nanostructures. Her work explores how synthesis conditions influence material performance, contributing to advancements in nanotechnology and energy-related applications. Dr. Kiprotich has authored numerous peer-reviewed publications in reputable journals, with her research widely cited in the field of materials science. As both a scholar and academic leader, she continues to advance research, innovation, and teaching in physics and related disciplines.